Journal of ELECTRONIC MATERIALS, Vol. 47, No. 5, 2018
https://doi.org/10.1007/s11664-018-6118-8

Synthesis, Characterization and Applications of Ethyl Cellulose-Based Polymeric Calcium(II) Hydrogen Phosphate Composite

FARUQ MOHAMMAD,[1,3] TANVIR ARFIN,[2] and HAMAD A. AL-LOHEDAN[1]

1.—Surfactant Research Chair, Department of Chemistry, College of Science, King Saud University, P.O. Box 2455, Riyadh 11451, Saudi Arabia. 2.—Environmental Materials Division, CSIR-National Environmental Engineering Research Institute (CSIR-NEERI), Nehru Marg, Nagpur, India. 3.—e-mail: fmohammad@ksu.edu.sa

The present report deals with the synthesis, characterization and testing of an ethyl cellulose–calcium(II) hydrogen phosphate (EC–$CaHPO_4$) composite, where a sol–gel synthesis method was applied for the preparation of the composite so as to test its efficacy towards the electrochemical, biological, and adsorption related applications. The physical properties of the composite were characterized by using scanning electron microscopy (SEM), ultraviolet–visible (UV–Vis) spectroscopy, and fourier transform-infrared (FTIR) spectroscopy. On testing, the mechanical properties indicated that the composite is highly stable due to the cross-linked rigid framework and the enhanced interactions offered by the EC polymer supported for its binding very effectively. In addition, the conductivity of EC–$CaHPO_4$ is completely governed by the transport mechanism where the electrolyte concentration has preference towards the adsorption of ions and the variations in the conductivity significantly affected the material's performance. We observed an increasing order of KCl > NaCl for the conductivity when 1:1 electrolytes were applied. Further, the material was tested for its usefulness towards the purification of industrial waste waters by removing harmful metal ions from the samples collected near the Aligarh city, India where the data indicates that the material has highest affinity towards Pb^{2+}, Cu^{2+}, Ni^{2+} and Fe^{3+} metal ions. Finally, the biological efficiency of the material was confirmed by means of testing the antibacterial activity against two gram positive (*staphylococcus aureus and Bacillus thuringiensis*) and two gram negative bacteriums (*Pseudomonas aeruginosa and Patoea dispersa*). Thus, from the cumulative study of outcomes, it indicates that the EC–$CaHPO_4$ composite found to serve as a potential smart biomaterial due to its efficiency in many different applications that includes the electrical conductivity, adsorption capability, and antimicrobial activity.

Key words: Surface modification, ethyl cellulose, $CaHPO_4$, organic–inorganic polymer composite, antibacterial activity, heavy metal adsorption

INTRODUCTION

Recent advancements in materials science and nanotechnology fields present a wide range of interest towards the development of nano-scale materials with many advanced applications, which include solar cells, energy conversion and storage, biomedicine, sensors, catalysis, engineering and construction.[1–3] Such advancement and mobility in the concepts of materials science and nanotechnology is made possible only due to the development of novel synthesis methods and advanced characterization tools denoting their significant contribution and potential applications.[4] Also, composite

(Received October 3, 2017; accepted February 1, 2018; published online March 2, 2018)

membranes, made up of inorganic nanomaterials when applied for filtration purposes, the membrane properties should be fine-tuned in such a way that it can allow only particular moieties to pass through them while blocking others. In that view, one approach to alter the fundamental properties is by forming composites that involve organic, inorganic or polymer substrates. Since the organic and inorganic materials individually are efficient enough to suit all applications because of their intrinsic properties, such as the solubility, mechanical, chemical and thermal stabilities, in order to overcome these limitations inorganic–organic composite membranes are introduced.[5] Thus, the formed composite membranes can easily find applications in various sectors of filtration and/or separations that include the chemical and petroleum industries, waste water treatment, fuel cells, cell sorting and stem cell technology etc., as these applications are authorized for high thermal, chemical and mechanical resistivity.[6–8] The other properties such as availability, stability, flexibility and eco-friendly nature are also useful and quite beneficial where the polymers serve as important materials for the preparation of composites with outstanding separation performance and adaptability to environmental changes.

Cellulose is a material that exhibits promising mechanical and biodegradable properties along with hydrophobicity, biocompatibility, and sustainability.[9,10] The derivatives of cellulose are generally ethers of alkali or hydroxyalkyl groups, which are randomly replaced to a limited extent on the three available hydroxyl groups of individual anhydroglucose unit.[11] Among many different alkyl derivatives of natural celluloses, ethyl cellulose (EC) is generally applied as a food packaging material due to its stability, non-toxic nature, and antimicrobial behavior towards the microorganisms.[12] So, in order to preserve food products for maintaining better quality, recent techniques of effective packaging generally include oxygen scavengers and antioxidant additives.[13] Further, in recent years, the increased interest towards the conductivity of EC polymer from both fundamental research, as well as the practical application point is due to its critical role as an electrically conductive ionomeric material. The unique features of EC polymer are the preservation of high electrical conductivity at ambient and sub-ambient temperature conditions, and in addition, the enhancement in the electro active character is due to its electrochromic nature supported by the active chemical surface.[14,15]

By taking advantage of the composite technology principles and the inbuilt properties of EC polymer, the present work is aimed to develop a solid polymer composite system that has multiple application sites. For that, we prepared the polymer-inorganic composite by following the sol–gel approach where the EC polymer served as a binder to the calcium(II) hydrogen phosphate ($CaHPO_4$) material and further tested for the electrochemical, biological, and environmental-related applications. We started with the physical characterization of the composite followed by its efficacy testing towards the ionic conductivity, antibacterial activity, and metal ion adsorption potency. Although our earlier reports dealing with other EC-based composites,[15] the present report extends our understanding of the EC-based hydrogen phosphate composites so as to employ them in novel application areas, i.e. in the present case, for the separation of harmful metal ions in real-time industrial waste water samples collected from Aligarh city, India.

EXPERIMENTAL

Synthesis of EC–Ca(II)HPO_4 Composite

For the synthesis of the EC–Ca(II)HPO_4 composite, we applied the same method earlier developed by Arfin et al.[15] Briefly, about 0.2 M each of $CaCl_2$ and dipotassium hydrogen orthophosphate (K_2HPO_4 solutions were mixed together, followed by the drop-wise addition of dilute HCl (35.4%) with constant stirring using the magnet for 10 mins. When we adjusted the pH of mixture to 1.0 and at room temperature, the formation of precipitate was observed which was allowed to keep for 24 h. After the required period, the solution was centrifuged to separate out the precipitate, washed the precipitate with deionized water 2–3 times, and dried the precipitate at 90°C in a heating furnace. The dried precipitate was grounded to fine powder with the help of a mortar and pestle, sieved through 85 mm sieve to obtain the $CaHPO_4$ compound as mentioned below:

$$CaCl_2 + K_2HPO_4 \rightarrow CaHPO_4 + 2KCl$$

For the bonding of $CaHPO_4$ with EC polymer, both the compounds were mixed and grounded properly in a mortar continuously for at least 4 h, followed by heating the mixture in a hot air oven maintained at 80°C for 1 h for an equilibrium reaction. This heating process for the equilibrium was practised in order to synthesize the final product with high mechanical and chemical stabilities and we found that the final composite with 25° of EC polymer seems to be of highest mechanical strength as compared to other combinations. For the testing, the tablets were prepared by taking a 1:3 ratio of EC and $CaHPO_4$ powders.

The following preliminary structure can be anticipated for the final composite:

$$Ca(HPO_4)\cdot nH_2O + [C_6H_7O_2(OC_2H_5)_3] \rightarrow Ca(HPO_4)\cdot[C_6H_7O_2(OC_2H_5)_3]\cdot nH_2O$$

where '*n*' shows the number of hydrated H_2O molecules.

Conductivity Measurements

For the electrochemical measurements, the equipment employed was the same as mentioned in our earlier publications.[16] Briefly, the synthesized material was first inserted in-between two glass half-cells having a volume each of 20 mL and active material area of 60.13 mm^2. For the analysis, two different electrolyte solutions (KCl and NaCl) with a range of concentrations using deionized water as solvent was prepared. A stirrer with a stirring rate of 600 rpm was maintained at the base of individual half-cell for decreasing the concentration-polarization effects. Also, the conductivity was recorded by varying the solution pH in the range of 5.5–6, while the temperature in the range of $(5 \pm 50) \pm 0.2°C$ using the conductivity meter (VSI-05, Mohali). For the data, each experiment was repeated thrice and the average of all these values was used as the final measurement.

Testing of Real-Time Aqueous Samples

Heavy metal ions containing samples gathered from various industrial sites of Aligarh city in India were analyzed by applying the columns of EC–$CaHPO_4$ with flame atomic absorption spectrophotometer (FAAS). For the analysis, the collected specimens were first filtered followed by acidification to pH 2 and then subjected to the prescribed method. For that, a solution of 500-1000 mL with pH of around 6.0 prepared with HCl was vent through a column at a flow rate of 5 mL/min. Now the metal ion(s) that were adsorbed onto the porous sites of the EC–$CaHPO_4$ composite was eluted using 5 mL of 2 M HNO_3 in acetone solution at a flow rate of 2 mL/min. Afterwards the collected eluent was subjected to FAAS analysis for the qualitative and quantitative determination of metal ions.[17]

Measurement of Antibacterial Activity

The antibacterial activity of EC–$CaHPO_4$ composite was tested by applying the well-diffusion method against two gram positive (*Staphylococcus aureus* and *Bacillus thuringiensis*) and two gram negative (*Pseudomonas aeruginosa* and *Pantoea dispersa*) bacteriums and further compared with the standard drug ampicillin.[15] Here, Ampicillin was applied as a positive control and dimethyl sulfoxide (DMSO) as negative. For the treatments, the cultures of actively dividing bacterial cells of about 10^6 CFU/mL volume was vaccinated in flasks which already contain sterilized nutrient broths with varying concentrations of our EC–$CaHPO_4$ material. These flasks were shaken at a speed of 160 rpm at $36 \pm 2°C$ on an orbital shaker and the minimal inhibitory concentrations (MICs) were recorded through the use of the broth dilution method. For the analysis, each measurement was repeated thrice for the suitable outcomes.

Physical Characterization

A UV-1800 spectrophotometer (Shimadzu) was employed for the ultraviolet–visible (UV–Vis) spectroscopic analysis, where an aqueous suspension of EC–$CaHPO_4$ material was tested by employing deionized methanol as the standard reference. The Fourier transform-infrared (FTIR) spectra of the EC–$CaHPO_4$ composite at different stages of its formation were recorded by using an Alpha-FTIR spectroscopy (Bruker) instrument. The samples were analyzed by the KBr pellet method with a determination of 4 cm^{-1} in 32 scans at ambient temperature in the wavenumber range of 4000–400 cm^{-1}. The surface morphology of the material was carried out using a Quanta FEG 250 environmental scanning electron microscope (ESEM). An X' Pert PRO analytical diffractometer (PW-3040/60 with Cu Kα radiation λ = 1.5418 Å) at a scan rate of 2°/min was used for x-ray diffraction (XRD) analysis. The porosity of the composite for the pore size analysis was examined by the mercury intrusion porosimetry (Micromeritics, Model Autopore IV 9500V). The quantitative separations of metal ions were analyzed by using the FAAS instrument (GBC-932-Plusflame atomic absorption spectrometer).

RESULTS AND DISCUSSION

Physical Characterization

The UV–Vis spectral analysis of EC and EC–CaHPO4 composite in the mid ultraviolet range of 200–250 nm is compared and shown in Figure 1. For the analysis, each sample was scrutinized individually at ambient temperature with the wavelength at high absorption of 208 nm. It was noted that the absorption peak for both compounds was around 210 nm, which attributed to the π–π^* transitions in small electronically conjugated domains of the groups of EC molecules.[15] The observation of peak for both the compounds at the same position (no peak shift) provides the confirmation that there are not changes getting occurred to the bonds of EC matrix even after conjugating with the $CaHPO_4$ complex molecules. In addition, the spectrum of the EC–$CaHPO_4$ composite has a small absorption peak around 250 nm which corresponds to the similar π–π^* transition of the PO_4 groups of the $CaHPO_4$ compound.[18] Thus, from the UV–Vis analysis, the spectrum of the EC–$CaHPO_4$ composite maintains the mixed absorption peaks from both the groups of EC and $CaHPO_4$, meaning that the composite formation reaction is a success.

In order to fully understand the interaction or extent of bonding between two or more components of the same composite, the FTIR spectroscopic technique is usually employed. Figure 2 shows the comparison of the FTIR spectra between EC, $CaHPO_4$ and EC–$CaHPO_4$ composite; the common peaks between pure EC and EC–$CaHPO_4$ composite observed around 3300 cm^{-1}, 2890 cm^{-1}, 1400 cm^{-1},

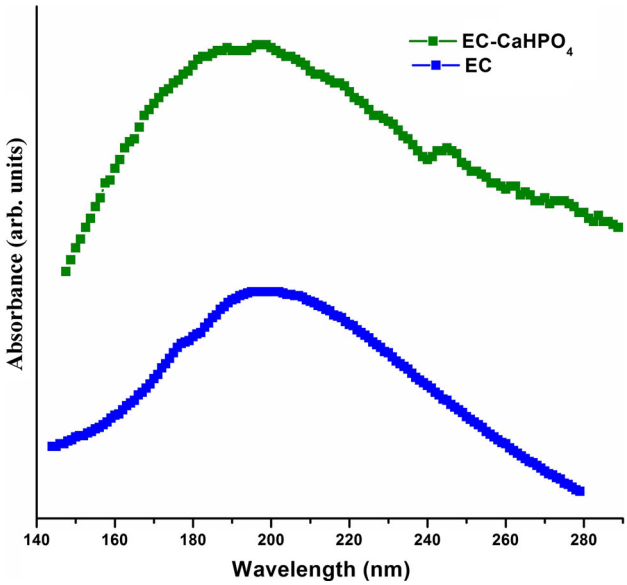

Fig. 1. Comparison of the UV–Vis spectroscopic analysis between EC polymer and EC–$CaHPO_4$ composite.

and 1110 cm^{-1} corresponds to the -OH, -CH stretching, $-CH_3$ and $-CH_2$ bending vibrations, respectively. Also, the C-O-C stretching vibration of the cyclic ether of EC is strong and appeared around 1110 cm^{-1} getting slightly reduced to 1090 cm^{-1} due to the composite formation.[19,20] Similarly for the $CaHPO_4$, the bands at 930 cm^{-1} and 610 cm^{-1} ascribed to the symmetric and asymmetric vibrations of PO_4^{3-} group are shifted to 1010 cm^{-1} and 630 cm^{-1} (respectively) after bonding with the EC matrix. In addition, the P-O symmetric stretching and asymmetric bending vibration can be found around 1380 cm^{-1} and 750 cm^{-1} for both the samples can further provide evidence for the successful conjugation of the HPO_4^{2-} groups to the EC matrix.[18] From the cumulative FTIR analysis, it is evident that the EC–$CaHPO_4$ material maintains the common bands of both EC and $CaHPO_4$ compounds, which further indicates that the final composite is a successful mixture of organic and inorganic molecules.

Figure 3 shows the surface/morphological analysis of EC–$CaHPO_4$ material at different stages of its formation where the latter image (Fig. 3b) indicates the formation of uniform porous patches in the matrix of EC polymer. Here, the pores are seems to be in the form of identical capillaries, which are distributed all over the surface covering the $CaHPO_4$ core. Since for the composite, the covering of a porous and very thick EC layer onto the solid surface of $CaHPO_4$ is particularly useful for the conductivity and adsorption related applications where the ions and adsorbing agents can make use of the porous space (respectively). Further, for the mentioned applications, the entry and exit portions should not be affected in comparison to the pore radius so as to accommodate the conductive ions or adsorbing agents within the moieties. In that view, the morphology provided by our EC–$CaHPO_4$ composite material is expected to offer the steady equilibrium phase by taking advantage of both the EC matrix and $CaHPO_4$ properties to exchange the charge density and mobile species easily. However, the microscopic image (Fig. 3a) of uncoated $CaHPO_4$ seems to maintain the heterogeneous surface with the absence of any visible phase separations, pores or holes at the surface. The maintenance of heterogeneous surface can be advantageous for the strong bonding of the EC matrix to the surface of $CaHPO_4$ so as to allow maximum mechanical strength to the final composite.[21,22]

The particles size in the EC–$CaHPO_4$ composite examined using the mercury porosimetry is shown in Fig. 4 where it can be seen that the particles appeared to macro-porous in size with a single peak distribution centred at 142.95 nm. The formation of the final composite in that lower size range is mainly attributed to the use of sol–gel technique during the preparation of the composite.

The average crystalline size (D) can be determined through the application of Scherrer equation given below[23]:

$$D = \frac{K\lambda}{\beta \cos\theta} \quad (1)$$

where K is the shape factor and its value is 0.9, λ is the wavelength, β is the full width and θ is Bragg's angle. The comparison of the XRD patterns for the EC–$CaHPO_4$ composite with that of pure EC and $CaHPO_4$ are shown in Fig. 5. From the figure, the observation of two major peaks around 11° and 20° for the pure EC material confirms for its amorphous nature where the former peak follows the interlayer distance of the ordered cellulose chains while the second peak ascribes to interchange distance.[24] Similarly, for the $CaHPO_4$ compound, several sharp peaks at 28°, 32°, 46°, 55°, 58°, and 78° were found with standard graphics of $CaHPO_4{\cdot}2H_2O$ (reference code: 00-001-0395),[25] which further indicates the formation of $CaHPO_4{\cdot}2H_2O$ compound's crystalline structure to be in the triclinic unit cell phase.[18] However, for the EC–$CaHPO_4$ composite, the XRD peaks were observed to be a combination of peaks from both EC and $CaHPO_4$ groups, i.e. the observed peaks are around 20°, 28°, 32°, 46°, 55°, 58° and 78°. The observation of both group peaks in addition to the absence of other trace elemental peaks further confirms for the successful encapsulation of $CaHPO_4$ with the EC polymer and also the efficiency of the synthesis approach. Thus, the straight base line and the sharp peaks of the diffractogram confirm that the EC–$CaHPO_4$ has good crystalline property, which is further responsible for the structural quality.

For determining the lattice parameters of the EC–$CaHPO_4$ composite, the XRD peak of crystal at

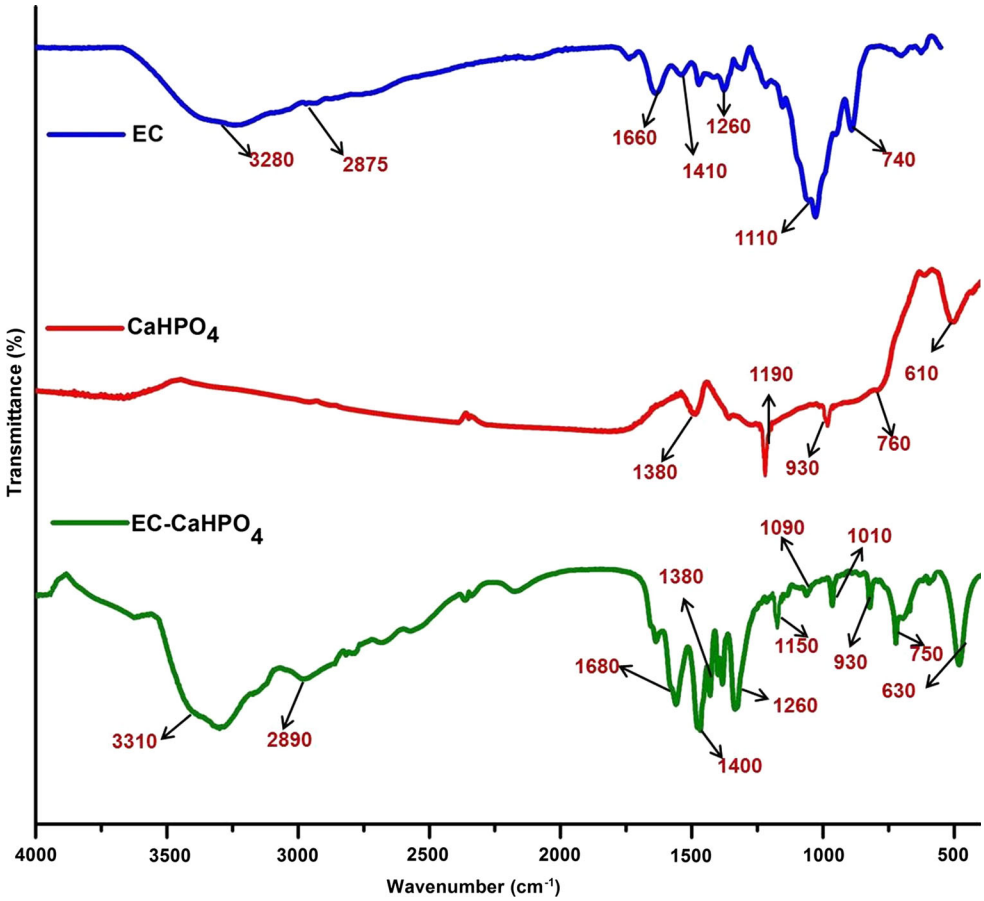

Fig. 2. Comparison of the FTIR spectra of EC and $CaHPO_4$ materials with that of the EC–$CaHPO_4$ composite.

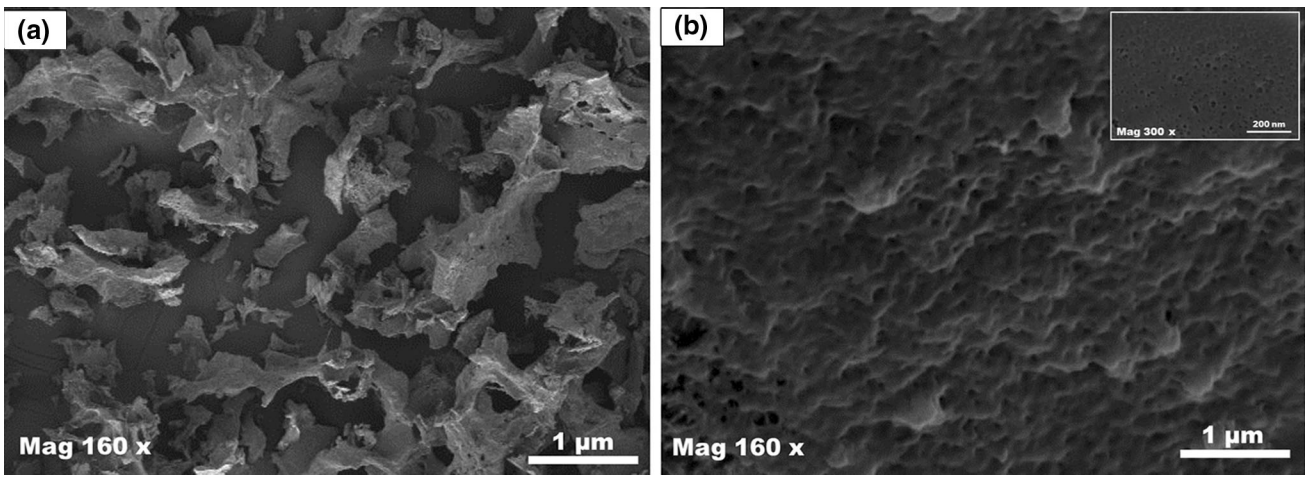

Fig. 3. Comparison of the SEM images of (a) $CaHPO_4$ and (b) EC–$CaHPO_4$ composite.

32° was selected. The lattice parameter was obtained by using the following Eq. 2,

$$d_{hkl} = \frac{\lambda}{2\sin\theta} \quad (2)$$

where d_{hkl} is the distance between the crystal planes of (h k l); λ is the wavelength, θ is the diffraction angle of the crystal plane (h k l); (h k l) is the crystal plane index; and a, b, and c are the lattice parameters.

Based on the calculation of the XRD peak broadening, the average crystalline size of EC–$CaHPO_4$ composite observed to be 20 nm. The lattice parameters, a, b, and c for the material were also

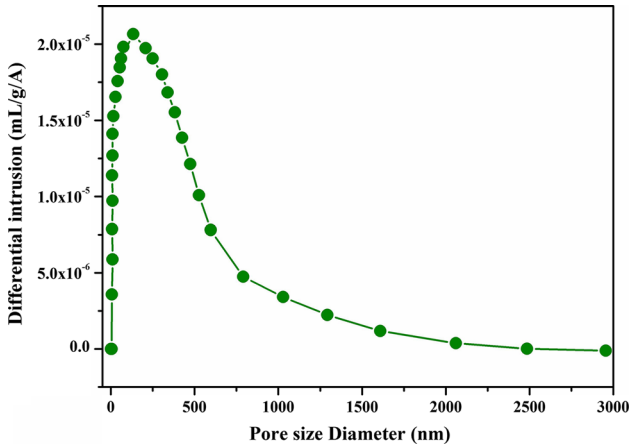

Fig. 4. Pore size distribution of the EC–$CaHPO_4$ composite.

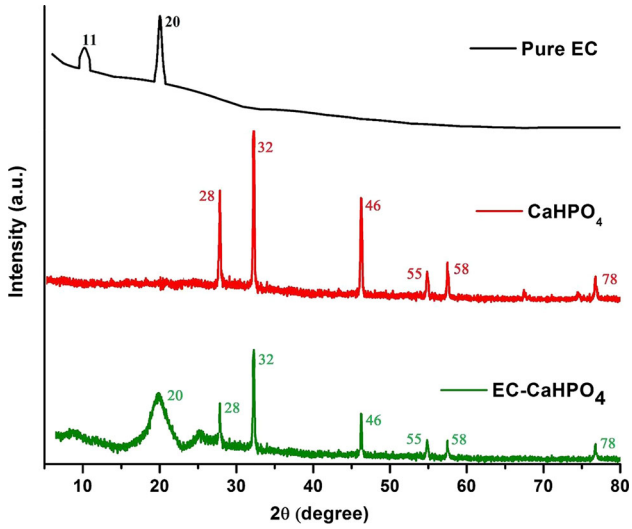

Fig. 5. Comparison of powdered XRD of the EC–$CaHPO_4$ composite with that of pure EC and $CaHPO_4$ complex.

calculated to be 6.82 nm, 6.50 nm, and 6.80 nm, respectively. Thus the diffraction pattern for the material revealed the formation of a single phase in the detection limit of powdered XRD.

Conductivity Studies

In general for any material, the conduction phenomenon within the pores serves as a significant factor for the transport properties, while the electrical resistance estimation permits for the understanding of electrolyte conductivity within the pores. Figure 6 describes the ambient temperature conductivity behavior of the EC–$CaHPO_4$ composite when tested against two different electrolyte solutions having concentration change. One can see from the figure that the conductivity of EC–$CaHPO_4$ composite is influenced by the number of ions, i.e. the solution conductivity where it was noted that more conducting power was measured for a solution with a larger number of

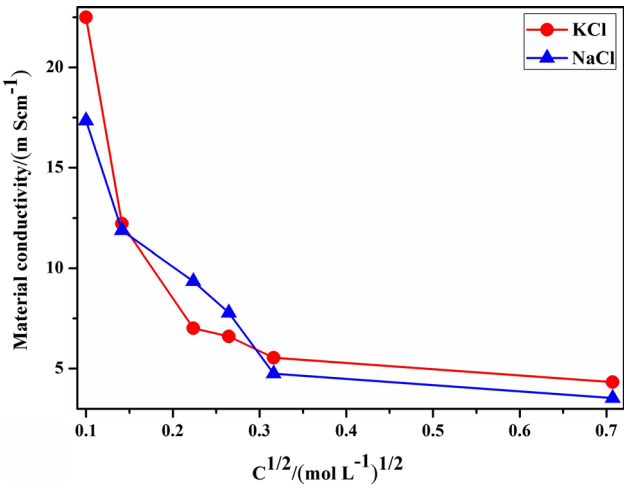

Fig. 6. Plot of material conductivity versus concentration for the EC–$CaHPO_4$ composite when 1:1 electrolyte was used at 25 ± 0.1°C temperature.

ions, as compared to the one with fewer ions of the same concentration and temperature. This is further influenced by the degree of dissociation towards the ions number from an electrolyte solution where strong electrolytes such as KCl and NaCl have a higher degree of dissociation. These electrolytes exhibit ionic properties even in the solid state conditions and have a 100% dissociation rate. Further, the interaction of composite with solvent results in the disintegration of potential electrolytes very quickly and the degree of dissociation in such case gets increased due to an increased dilution and so the number of ions available for conduction also is increased. This is the reason for the observation of an increased conductivity with that of electrolyte concentration at all cases of our study (Fig. 6).[26,27] Also, with respect to the hydrated radii size of the respective ions, the conductivity of the EC–$CaHPO_4$ composite for univalent electrolyte solution generally decreases in the particular order $K^+ > Na^+$. The reason for the observation such activity may be due to the fact that the ions with lesser hydrated radii were seems to get in the pores of material very conveniently, which further results in the higher absorption rates.[28,29]

The Arrhenius expression shows the temperature dependence of conductivity

$$\sigma T = \sigma_0 \exp\left(\frac{E_a}{\kappa T}\right) \quad (3)$$

where σ_0 is the pre-exponential factor, T the temperature, κ the constant and E_a the activation energy. For getting the activation energy, the conductivity data were empowered to the equation. The temperature depends on the conductivity and follows the Arrhenius equation as mentioned in Fig. 7 and it was noted that the other respective samples also show the same conductivity behavior. It was apprehensive to state that the temperature is the key factor on which

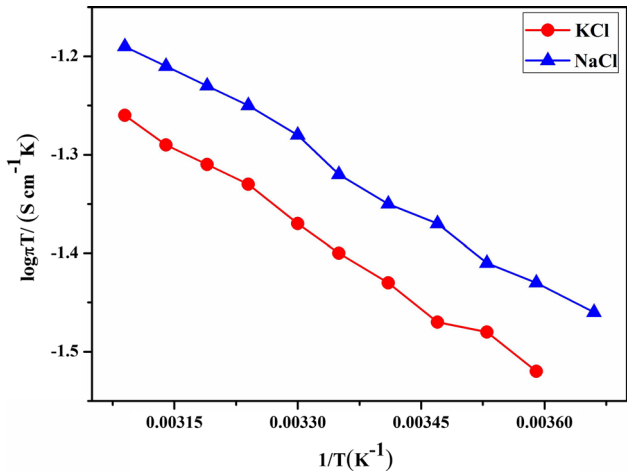

Fig. 7. Plot of material conductivity versus temperature for the EC–$CaHPO_4$ when 0.5 M of 1:1 electrolyte at (25–50) ± 0.1°C temperature was applied.

the conductivity for univalent electrolytes is strongly dependent where the increase in temperature caused the conductivity to increase proportionally. The EC–$CaHPO_4$ is in the semi-conductor region as it is revealed by the value of conductivity, which lies within the order of 10^{-3} m S cm^{-1}.[15]

The linear regression method was employed to calculate the activation energy in terms of eV from the slope and the obtained values for the univalent electrolyte solution is shown in Table I. The observation of lower activation energy values for the material is due to the super-ionic nature in the underlying temperature zone. Also, the change in the activation energies for the composite with respect to the electrolyte concentration at ambient temperature conditions is shown in Fig. 8. From the figure, we observed an increased order of activation energy to be $K^{+>}$ Na^+ and the observation of such result may be due to the difference in the nature of solvent which is carried in conjugation with the specific electrolyte concentration and further responsible for sequencing of the crystallographic radii of the cation, i.e. an alkali metal.

pH Study

The electrolytes solution over the pH was used to test the pH response profile for the EC–$CaHPO_4$ material. Figure 9 depicts the extensive changes in the pH response by the material, where we found from the analysis of results that the potential seems to be constant in the range of 5.0–7.5 and some drifts were noticed beyond this range.[30] With further increase in the pH, a significant drop in the electrode potential was indicated for the material, and the observation of such results can be attributed to the development of hydroxyl complexes, which restrict the charge transfer processes in the composite. Overall, from this pH dependent electrode potential study, we noticed an improved potential for the EC–$CaHPO_4$ material at low pH conditions (below pH 7.5), which resembled the fact that the material is in good agreement with the formation of protonium ions, where the acidic protons gets readily absorbed by the composite material and co-ordinates to an increased degree of the protonation of phosphorus atoms of the phosphate. Thus, formed H_3O^+ ions at lower pH conditions significantly improves the charge transport processes across the layers of the composite and can be the operating mechanism for the observation of enhanced conductivity values.[30,31]

Environmental Applications

The practical efficacy of our developed composite was established by means of the adsorption of metal ions such as Pb^{2+}, Cu^{2+}, Ni^{2+} and Fe^{3+} in industrial waste water samples where the ability was tested by a five time examination approach and the values are depicted in Table II. The outcome of water examination of different samples with RSD < 5% helped for the pertinence of the approach where we found that the approach is by all accounts particular and exact which is clear from the standard deviation information.[32] The analysis of results provided in the table indicates that the EC–$CaHPO_4$ composite can serve as a better adsorbent bed for the discharge of harmful metal ions from the industrial waste water samples. Since the microscopic images provided in Fig. 3 indicates that the surface of the composite is rough and heterogeneous, where such morphology in general offers for an increased surface area for the adsorbing ions and increases the interaction between the adsorbate and adsorbent species.[33] Also, the porous nature of the material (Fig. 3b) enhances the localization of electron deficient metal ions into the stable wells of the EC matrix. Further, from the analysis of data, we found a slight difference in the quantity of metal ions that got adsorbed onto the adsorbent's surface, i.e. the EC–$CaHPO_4$ composite seems to have the highest affinity towards the Pb^{2+} ions as compared to the other metal ions of Cu^{2+}, Ni^{2+}, and Fe^{2+} and we are not really sure at this stage for the observation of such random results. However, one reason for the observation of highest affinity towards Pb^{2+} by the EC–$CaHPO_4$ composite may be due to the matching of size and surface energy factors, as similar results were observed when Teff straw (*Eragrostis tef*) from the agricultural waste was used as an adsorbent bed for the separation of metal ions (Cr, Cd, Pb, Ni, and Cu) from the waste water streams of textile industries.[34] Thus, from the analysis of results it can be concluded that the EC–$CaHPO_4$ composite can serve as a better adsorbent bed for the sustainable discharge of harmful

Table I. Activation energies of conduction for the EC–$CaHPO_4$ composite when 0.5 M of 1:1 electrolyte at (25–50) ± 0.1°C temperature was used

Electrolyte (mol/L)	Activation energy (eV)
KCl	0.025
NaCl	0.017

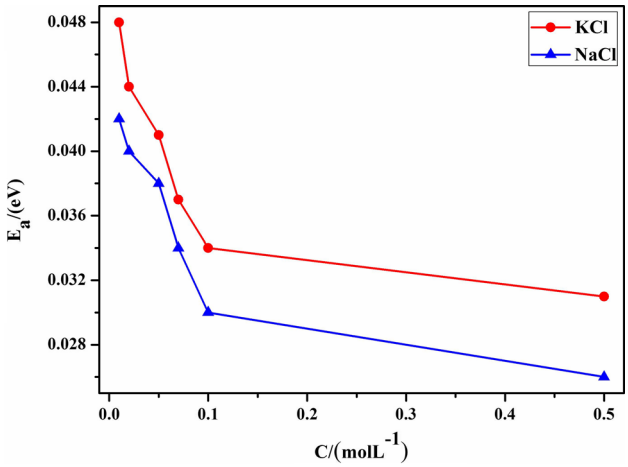

Fig. 8. Plot of activation energy versus concentration for the EC–$CaHPO_4$ using 1:1 electrolyte at 25 ± 0.1°C.

metal ion like Pb^{2+} from the industrial waste water and other environmental samples.

Investigation of Biological Activity

The biological activity testing for the EC-$CaHPO_4$ composite provided the evidence that the material has some antibacterial activity as it responded very well by generating significant zones of inhibition (ZoI). The material was tested against two gram positive and two gram negative bacteriums where the average of the three corresponding readings was recorded (Table III). The ZoIs are taken to be as 20 mm, where the inhibition activity is found to be excellent and is in the range of 10–12 mm, low at 7–9 mm and non-critical underneath 7 mm. Similarly, for any smart material and the microorganisms examined, the values of MICs are generally in the range of 36–55 μg/mL.[35] However, for our composite, the values of ZoIs tested for *Bacillus thuringiensis*, *Staphylococcu aureus, Pseudomonas aeruginosa, Pantoea dispersa* were found to be 28 mm, 21 mm, 24 mm and 22 mm (respectively) at the corresponding MICs of 30 μg/mL, 36 μg/mL, 55 μg/mL, and 45 μg/mL, respectively (Table IV). The comparison of our observed results of ZoIs and MICs with the literature data, it is indicated that the composite has potentials to serve as an effective antibacterial where its components are not that toxic to nature and so the sustainability issue can be conceded easily.

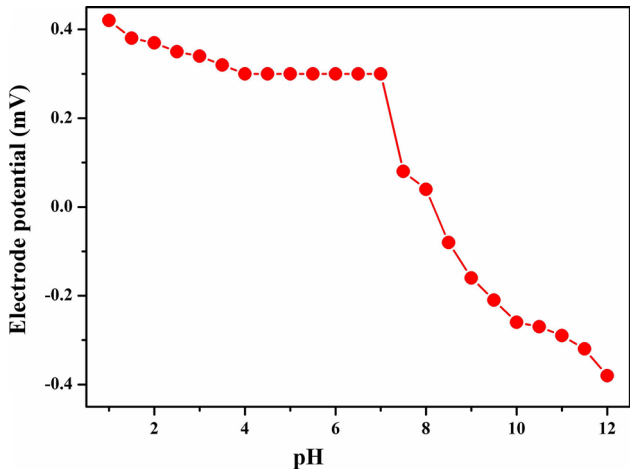

Fig. 9. Effect of pH of KCl solution (1×10^{-2} mol/L) on the potential response of the EC–$CaHPO_4$ composite.

For the composite, the reflection of antibacterial activity is mostly linked to the existence of EC matrix and Ca complex, as both of the elements contributes mostly for the bacterial and fungal inhibition by means of disrupting the cellular metabolic processes.[36,37] The presence of EC as a natural polymer in the composite is responsible for the cellular adhesion, while the porous structure enhances the growth and supports more for the permeability of the bacteria or fungi inside the polymer (Fig. 3b). Also, the complexation of EC with Ca(II) complex greatly reduces the polarity by means of partially sharing some of its electrons between the two components. The marriage between these two components greatly enhances the lipophilic nature of Ca ions, meaning that higher interactions between the composite and the microorganisms are expected which allows the particles to cross the lipid bilayer easily and so the bacterial cell growth is significantly reduced.[36] The outcome exhibits that the EC–$CaHPO_4$ is more dynamic against all tested bacterial strains than ampicillin drug, which was utilized as a controlled approach.[14,15] Similarly, the presence of Ca(II) complex in the composite also restricts the growth of bacteria by inhibiting the formation of biofilms and lactic acid production and further decay.[37] Finally, it can be indicated from our studies that the composite can be applied as a potent antibacterial agent directly or in combination with other drugs for the controlling of bacterial activity in moderate ranges.

On comparison of the results provided by EC–$CaHPO_4$ composite with that of our earlier work on EC–$MgHPO_4$,[21] EC–$SnHPO_4$,[38] and EC–$NiHPO_4$[39] composites we believe that the present material is far superior where the EC–$CaHPO_4$ composite exhibited significant effects in all the applications of electrochemical, antimicrobial, and adsorption. From the electrical conductivity studies, we observed a highest of 23 m S cm^{-1} for the EC–$CaHPO_4$ composite as compared against

Table II. Determination of Pb^{2+}, Cu^{2+}, Ni^{2+} and Fe^{3+} in different industrial samples on the column of EC–$CaHPO_4$

Sample	Method	Pb^{2+a} (ppb) (% RSD)	Cu^{2+a} (ppb) (% RSD)	Ni^{2+a} (ppb) (% RSD)	Fe^{3+a} (ppb) (% RSD)
M_1	Direct[b]	16 (1.5)	7 (3.4)	9.7 (1.1)	2.2 (1.7)
	SA[c]	19 (2.5)	10 (2.9)	9.5 (1.0)	1.2 (1.2)
M_2	Direct[b]	15.0 (0.7)	6.4 (1.2)	2.5 (3.0)	4.2 (3.2)
	SA[c]	12.9 (2.3)	9.0 (0.29)	3.8 (2.5)	4.9 (1.9)
M_3	Direct[b]	18.8 (0.18)	3.1 (2.2)	2.88 (2.3)	3.7 (2.9)
	SA[c]	20.0 (3.4)	3.9 (3.8)	3.9 (1.0)	4.0 (2.2)

M1 (Talanagri, Aligarh), M2 (Ramghat road, Aligarh), M3 (Abdul kareem, Aligarh)% *RSD* relative standard deviation.[a]Average of three replicates determinations.[b]Recommended procedure applied without spiking.[c]Recommended procedure after spiking (standard addition method).

Table III. Comparison of the ZoIs of EC–$CaHPO_4$ composite with that of ampicillin

	Zone inhibition (mm)			
	Gram positive		Gram negative	
Treatment (100 μg/mL)	*B. Thuringiensis*	*S. Aureus*	*P. Dispersa*	*P. Aeruginosa*
EC–$CaHPO_4$	28	21	24	22
Ampicillin	26	21	23	20

Table IV. MIC of EC–$CaHPO_4$

Microorganisms	MIC (μg/mL)
P. Dispersa	45 ± 7
P. Aeruginosa	55 ± 5
B. Thuringiensis	30 ± 4
S. Aureus	36 ± 8

Amp: ampicillin, a standard antibiotic used during the experiment. Minimum inhibition concentration (MIC), mean ± SD of each triplicate value.

the other three composites of EC–$SnHPO_4$ (18 m S cm^{-1}), EC–$NiHPO_4$ (19 m S cm^{-1}), and EC–$MgHPO_4$ (9 m S cm^{-1}). Similarly, the antibacterial effect offered by the EC–$CaHPO_4$ composite is found to be better than the other three EC-based composites where we were able to achieve considerable ZoIs even with the usage of minimum concentrations. Finally, the present composite was also found to be effective by means of serving as an adsorbing agent for the removal of metal ions (some are toxic too) from the industrial waste water streams, where the other EC-based complexes are not tested. Moreover, considering the toxicity effects of Sn and Ni in the EC–$SnHPO_4$ and EC–$NiHPO_4$ composites (respectively), the EC–$CaHPO_4$ composite is no way toxic to humans and to the environment and so in that way the point of sustainability can be resolved easily.

CONCLUSION

In summary, the current work describes about the synthesis, characterization and applications of the EC–$CaHPO_4$ composite for its conductivity, adsorption and antibacterial properties. We observed from the analysis of results that the composite has enhancement in the properties of conductivity, surface adsorption, and antibacterial activity as against the individual components of the same composite, in addition to the other composites of EC–$SnHPO_4$, EC–$MgHPO_4$ and EC–$NiHPO_4$. We found that the activation energy values for 1:1 electrolytes predicted their mechanical stability which is high applicable for being handled at different range of pHs. The efficiency of this material as compared to other EC-based composites was estimated by involving the material for the removal of harmful heavy metal ions from industrial water samples collected from different areas. The flexibility of the smart biomaterial should be adapted for permitting it to be further used in the fields of filtration, sensors and medical. As a result, it can be confirmed that the EC–$CaHPO_4$ would turn as a most promising biomaterial for the development of efficient, eco-friendly and sustainable technologies where the conductive, adsorption and antimicrobial functionalities are specifically required.

ACKNOWLEDGEMENTS

The authors (F.M. and H.A.A.L.) are grateful to the Deanship of Scientific Research, King Saud

University for funding through Vice Deanship of Scientific Research Chairs program.

CONFLICT OF INTEREST

The authors declare that they have no conflict of interest with this work.

REFERENCES

1. K. Oksman, Y. Aitomäki, A.P. Mathew, G. Siqueira, Q. Zhou, S. Butylina, S. Tanpichai, X. Zhou, and S. Hooshmand, *Compos. Part A: Appl. Sci. Manuf.* 83, 2 (2016).
2. J.S. Borah and D.S. Kim, *Korean J. Chem. Eng.* 33, 3035 (2016).
3. J. Silvestre, N. Silvestre, and J. de Brito, *Mech. Adv. Mater. Struct.* 23, 1263 (2016).
4. T. Kosuge, K. Imato, R. Goseki, and H. Otsuka, *Macromolecules* 49, 5903 (2016).
5. G. Chen, W. Xua, and D. Zhu, *J. Mater. Chem. C* 5, 4350 (2017).
6. Y.V. Antipov, A.A. Kul'kov, and N.V. Pimenov, *Polym. Sci. Ser.* 58, 26 (2016).
7. T. Miyazaki, A. Sugawara-Narutaki, and C. Ohtsuki, *Front. Oral Biol.* 17, 33 (2015).
8. H.C. Yang, J. Hou, V. Chen, and Z.K. Xu, *J. Mater. Chem. A* 4, 9716 (2016).
9. S.A. Khan, S.B. Khan, T. Kamal, A.M. Asiri, and K. Akhtar, *Recent Pat. Nanotechnol.* 10, 181 (2016).
10. F. Mohammad, H.A. Al-Lohedan, and H.N. Al-Haque, *Adv. Mater. Lett.* 8, 89 (2017).
11. Y. Sun, Y. Hu, X. Zhu, H. Zou, Y. Sui, J. Xue, L. Yuan, J. Zhang, L. Zheng, D. Zhang, and Z. Song, *J. Electron. Mater.* 46, 6811 (2017).
12. M. Torkaman and F.Z. Kazemabadi, *Orient. J. Chem.* 33, 1976 (2017).
13. H. Tang, M. Liu, Y. Ma, Z. Du, Y. Zhan, and W. Yang, *J. Electron. Mater.* 46, 637 (2017).
14. S.S. Sam, C.A. Ng, S.Y. Chee, N.Z. Habib, H. Nadeem, and W.P. Teoh, *IOP Conference Series: Earth and Environmental Science*, vol. 67, (2017), p. 012005.
15. F. Mohammad, T. Arfin, and H.A. Al-Lohedan, *Mater. Sci. Eng. C* 71, 735 (2017).
16. T. Arfin and Rafiuddin, *Electrochim. Acta* 56, 7476 (2011).
17. T. Arfin, R. Bushra, and F. Mohammad, *Graphene Technol.* 1, 1 (2016).
18. I.U. Khawaja, A. Choudhry, A. Mahmood, Z.A. Gilani, S.A. Shahid, and M. Farooq, *Optoelectron Adv. Mater.* 9, 1171 (2015).
19. S. Pandav and J. Naik, *J. Pharm.* 2014, 904036 (2014).
20. D.M. Patel, R.H. Jani, and C.N. Patel, *Int. J. Pharm. Inv.* 1, 172 (2011).
21. F. Mohammad, T. Arfin, and H.A. Al-Lohedan, *J. Ind. Eng. Chem.* 45, 33 (2017).
22. G.Y. Gor, P. Huber, and N. Bernstein, *Appl. Phys. Rev.* 4, 011303 (2017).
23. F. Mohammad, L. du Plessis, and T. Arfin, *X-Ray Diffraction: Structure, Principles and Applications*, ed. K. Shih (New York: Nova Science Publishers, 2013), p. 161.
24. L. Bruno, S. Kasapis, and P.W.S. Heng, *Carbohydrate Polym.* 88, 382 (2012).
25. A. Zhou, Q. Su, X. Li, and J. Weng, *Mater. Sci. Eng. A* 430, 341 (2006).
26. C.H. Lee, H.B. Park, Y.M. Lee, and R.D. Lee, *Ind. Eng. Chem. Res.* 44, 7617 (2005).
27. N. Schichte, C. Korte, D. Hesse, and J. Janek, *Phys. Chem. Chem. Phys.* 11, 3043 (2009).
28. A.P. Abbott, G. Capper, D.L. Davies, and R.K. Rasheed, *Chem. Eur. J.* 10, 3769 (2004).
29. J.A. Vega, C. Chartier, and W.E. Mustain, *J. Power Sources* 195, 7176 (2010).
30. Z. Gao, T.J. Bandosz, Z. Zhao, M. Han, and J. Qiu, *J. Hazard. Mater.* 167, 357 (2009).
31. M. Casciola, D. Capitani, A. Donnadio, V. Frittella, M. Pica, and M. Sganappa, *Fuel Cells* 9, 381 (2009).
32. A. Bondarev, S. Mihai, O. Pântea, and S. Neagoe, *Macromol. Symp.* 303, 78 (2011).
33. J.N. Cabrera, M.M. Ruiz, M. Fascio, N. D'Accorso, R. Mincheva, P. Dubois, L. Lizarraga, and R.M. Negri, *Polymers* 9, 331 (2017).
34. M.B. Desta, *J. Thermodyn.* 2013, 375830 (2013).
35. I. Wiegand, K. Hilpert, and R.E.W. Hancock, *Nat. Protoc.* 3, 163 (2008).
36. J.Y. Park, J.I. Kim, and I.H. Lee, *J. Nanosci. Nanotechnol.* 15, 5672 (2015).
37. L. Cheng, M.D. Weir, H.H.K. Xu, A.M. Kraigsley, N.J. Lin, S. Lin-Gibson, and X. Zhou, *Dent. Mater.* 28, 573 (2012).
38. T. Arfin and F. Mohammad, *Adv. Mater. Lett.* 6, 1058 (2015).
39. T. Arfin and F. Mohammad, *Innov. Corros. Mater. Sci.* 6, 1 (2016).